VT-GAN: Cooperative Tabular Data Synthesis using Vertical Federated Learning

Zilong Zhao* National University of Singapore Singapore z.zhao@nus.edu.sg

Aad van Moorsel University of Birmingham Birmingham, UK a.vanmoorsel@bham.ac.uk Han Wu*
University of Birmingham
Birmingham, UK
h.wu.6@bham.ac.uk

Lydia Y. Chen TU Delft Delft, The Netherlands lydiaychen@ieee.org

ABSTRACT

This paper presents the application of Vertical Federated Learning (VFL) to generate synthetic tabular data using Generative Adversarial Networks (GANs). VFL is a collaborative approach to train machine learning models among distinct tabular data holders, such as financial institutions, who possess disjoint features for the same group of customers. In this paper we introduce the VT-GAN framework, Vertical federated Tabular GAN, and demonstrate that VFL can be successfully used to implement GANs for distributed tabular data in privacy-preserving manner, with performance close to centralized GANs that assume shared data. We make design choices with respect to the distribution of GAN generator and discriminator models and introduce a training-with-shuffling technique so that no party can reconstruct training data from the GAN conditional vector. The paper presents (1) an implementation of VT-GAN, (2) a detailed quality evaluation of the VT-GAN-generated synthetic data, (3) an overall scalability examination of VT-GAN framework, (4) a security analysis on VT-GAN's robustness against Membership Inference Attack with different settings of Differential Privacy, for a range of datasets with diverse distribution characteristics. Our results demonstrate that VT-GAN can consistently generate high-fidelity synthetic tabular data of comparable quality to that generated by a centralized GAN algorithm. The difference in machine learning utility can be as low as 2.7%, even under extremely imbalanced data distributions across clients or with different numbers of clients.

KEYWORDS

Vertical Federated Learning, GAN, Privacy-preserving machine learning, Tabular data

Permission to make digital or hard copies of all or part of this work for personal or classroom use is granted without fee provided that copies are not made or distributed for profit or commercial advantage and that copies bear this notice and the full citation on the first page. Copyrights for components of this work owned by others than ACM must be honored. Abstracting with credit is permitted. To copy otherwise, or republish, to post on servers or to redistribute to lists, requires prior specific permission and/or a fee. Request permissions from permissions@acm.org.

1 INTRODUCTION

Tabular data, organized in rows and columns, is the most prevalent data format in industry [2]. Recent years has seen the proliferation of the use of synthetically generated tabular data as a privacy-preserving approach for data analysis and product development [9, 40]. State-of-the-art (SOTA) generation of synthetic tabular data utilises Generative Adversarial Networks (GANs) [20, 30, 42, 51, 55, 56]. However, training these GANs still requires direct access to all training data, raising an additional privacy concern if the data is coming from multiple sources.

Consider the following scenario. A regional e-commerce company and a bank hold separate information for a set of shared customers. Generating a synthetic dataset that combines the bank's customer income records with the customer's purchasing history in the e-commerce company would be highly beneficial to create more valuable data analysis and associated products. For instance, the bank can build a more robust prediction model for credit rating and the e-commerce company can build a more accurate recommendation system for its customers. In such cases, collecting and combining data from the bank and e-commerce company to train tabular GANs is not an option, because it involves sharing personal customer information across different organizations. In other words, we require a privacy-preserving approach to training the GAN, which avoids sharing data, and in this paper we consider Vertical Federated Learning (VFL).

Federated learning is a widely explored technique to train machine learning models on distributed data without sharing the data. Data remains in participating parties that hold data (known as clients) and learning is achieved by exchanging model information with a central party (also called the server), without sharing the data itself. In *Vertical* Federated Learning clients hold a local dataset with unique features pertaining to the *same* individuals or other identified subjects. This makes VFL particularly appropriate for various tabular data applications, while image or audio data would more naturally utilise *horizontal* federated learning, in which all clients have data with the same data feature structures. To train a prediction model under VFL [48], each client passes its local data through a bottom model (on the client side) and sends the output to a top model (on the server side) to calculate gradients. This ensures that local data is not directly accessed by any party except

1

^{*}Equal contribution

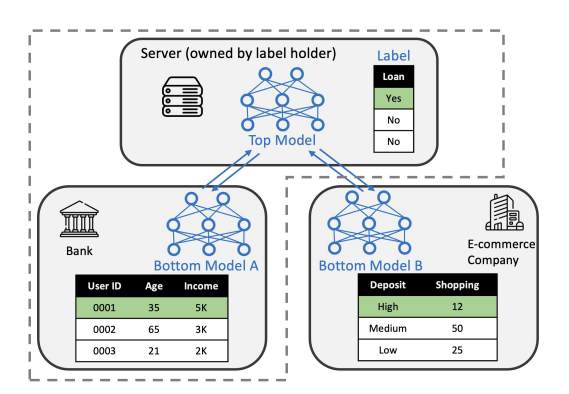


Figure 1: Traditional VFL architecture for prediction model.

the owning client, and only intermediate results are shared. Previous studies of VFL have concentrated on prediction models such as decision trees [49] and deep neural networks [44], there is no platform to train tabular GANs using VFL.

In this paper, we present a novel framework - VT-GAN which implements Vertical federated learning for Tabular GAN. The main challenge is to determine the bottom and top models, such that no data or personal information leaks from the individual clients, and the performance is close to that of a centralized model. By partitioning both GAN generator and discriminator models, placing pieces in each client and in the server, we assure that no data needs to be exchanged but that correlations between data from different clients can be captured by passing intermediate outcomes to the top model. Advanced tabular GANs utilize a technique called conditional GAN (CGAN)[51] and VT-GAN supports CGANs. Conditional GANs use a conditional vector (CV) to express conditions about the data considered in each learning step (e.g., limited to a specific gender). In VT-GAN, the server sends the conditional vector to all clients and the clients select data for their bottom model accordingly. However, a challenge arises when facilitating CGANs: the server may potentially deduce data characteristics in the clients based on the responses they receive from their bottom models, which are subsequently shared with the server. To mitigate this risk, in the end of each training round, VT-GAN implements a mechanism called training-with-shuffling in which all clients shuffle their local data using the same random seed. This ensures that the data after shuffling is still consistent across clients, but is not known to the server. Through this mechanism, the mapping between the CV and data index changes each round, making it impossible for the server to reconstruct the training data of clients.

We extensively evaluate VT-GAN using nine different partitions of the generator and discriminator neural networks between server and clients, and compare it to a centralized tabular GAN. The experiments are conducted on five commonly used tabular datasets in machine learning. We report on the machine learning (ML) utility and statistical similarity difference between the real and synthetic data. Results show that as long as the top model of the discriminator is large enough, VT-GAN performs comparably to the centralized tabular GAN baseline. In the data partition experiments, we discover that the more imbalanced the number of data columns across the clients, the lower the ML utility of the synthetic data. However, by shifting more neural networks of the generator from bottom to

top model, VT-GAN mitigates the negative effects of this imbalance. Additionally, we find that with an increasing number of clients, expanding the size of the generator neural network helps counteract the degradation in synthetic data quality. Finally, we evaluate the vulnerability of VT-GAN to Membership Inference Attacks (MIA). The full black-box MIA from [6] on VT-GAN generated synthetic data shows low success rate. Implementing Differential Privacy (DP) on VT-GAN can further lower the success rate of MIA, albeit at the expense of VT-GAN's performance. The main contribution of this study can be summarized as follows:

- We design the first of its kind distributed framework VT-GAN which incorporates state-of-the-art tabular GANs into vertical federated learning architecture.
- To accommodate conditional vector into VT-GAN training in a privacy-preserving manner, we devise the *training-with-shuffling* mechanism. We also propose a secure synthetic data publication strategy to mitigate the risk of inference attacks.
- We consider the semi-honest threat model and use it to motivate
 the design of VT-GAN. We qualitatively analyze the potential
 privacy risks in VT-GAN training. We experimentally evaluate
 the robustness of VT-GAN against Membership Inference Attack.
 Differential Privacy is also studied to implement on VT-GAN to
 provide protection.
- We extensively evaluate VT-GAN using five widely used machine learning datasets on eight evaluation metrics including the aspects of machine learning utility and statistical similarity. Results show that VT-GAN can stably generate high-fidelity synthetic data under extremely imbalanced data distribution across the clients. Optimal setup for VT-GAN is recommended under the constraints of computation resources, budgets, number of clients and data distributions across clients.

2 PRELIMINARIES AND MOTIVATION

VT-GAN enables training SOTA tabular GANs on VFL. In this section, we describe the preliminary of VFL and GAN.

2.1 Vertical Federated Learning

As depicted in Fig.1, a typical VFL system involves multiple clients, such as a bank and an e-commerce company, which possess distinct features for a shared group of users. It is important to note that in the illustration, the data instances of the clients have been aligned such that each row corresponds to the same individual across all clients. Data alignment across clients can be achieved by the Private Set Intersection (PSI) technique [7, 10], which is a common assumption used by VFL studies [16, 17, 49]. We also adopt it into our VT-GAN.

The goal of VFL is to train a common machine learning model using the features from all clients. In VFL, there are two types of models: top and bottom models as represented in Fig.1. During the training, each client passes their local data through the bottom model and sends the intermediate logits to the server. In practice, the server is typically managed by the client that holds the label column. As depicted by the dotted line in Fig.1, Bank is the label holder. The server horizontally concatenates the intermediate logits from all the clients and uses the concatenation as input for the top model. The top and bottom models are then updated using the

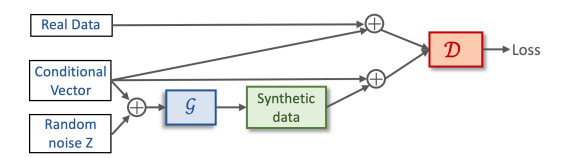


Figure 2: Conditional GAN (centralized).

Table 1: Summary of Notations

Notation	Description
\mathcal{G}^t , \mathcal{D}^t	top models of generator, discriminator
\mathcal{D}^s	conditional vector filter which runs on server
$\mathcal{G}_i^b, \mathcal{D}_i^b$	bottom model of generator, discriminator on client i
T_i	real tabular data held by client i
CV_p	conditional vectors constructed by client <i>p</i>
idx_p	data indices, the corresponding data contains
•	the indicating classes in CV_p
P_r	ratio vector, the ratio of number of features in each
	client to the total number of features across all the clients

gradients calculated from the discrepancy between the output of the top model and the label.

2.2 Tabular Generative Adversarial Network

Generative Adversarial Networks (GANs) [20] are a type of machine learning model designed to generate synthetic data that is similar to a given training dataset. They are composed of two parts: a generator (\mathcal{G}) and a discriminator (\mathcal{D}) as illustrated in Fig. 2. The generator is trained to generate synthetic data that is similar to the real data, while the discriminator is trained to distinguish between the synthetic data generated by the generator and the real training data. During the \mathcal{D} training step, the discriminator is trained separately by the synthetic data from generator and real data. During the \mathcal{G} training step, only the synthetic data is used. This process continues until the generator produces synthetic data that is indistinguishable from the real data.

To better indicate the category of generation (e.g., 'male' or 'female' in *gender* column), conditional GAN is well adopted for table synthesis [51, 55, 56]. Fig. 2 shows the structure of a conditional GAN (CGAN). CGAN controls the generation of synthetic data through the use of an auxiliary conditional vector (CV). The generator and discriminator are conditioned on the same CV. When using the real data to train discriminator, once a CV is given, the real data needs to sample one row of training data whose class is corresponding to the condition indicated in the CV. Feature engineering is another important tool for training tabular GANs. Before entering real data to \mathcal{D} , [30, 51, 55, 56] use mode-specific normalization [51] to encode continuous columns, one-hot encoding for categorical columns, mixed-type encoding [55] for column contains both categorical and continuous values.

3 METHODOLOGY

In this section, we begin by providing an overview of VT-GAN. We then justify the design of VT-GAN by introducing the privacy and security consideration.

3.1 VT-GAN Architecture

In this part, we begin by discussing the components of VT-GAN with an explanation of the design rationale for the structure, then

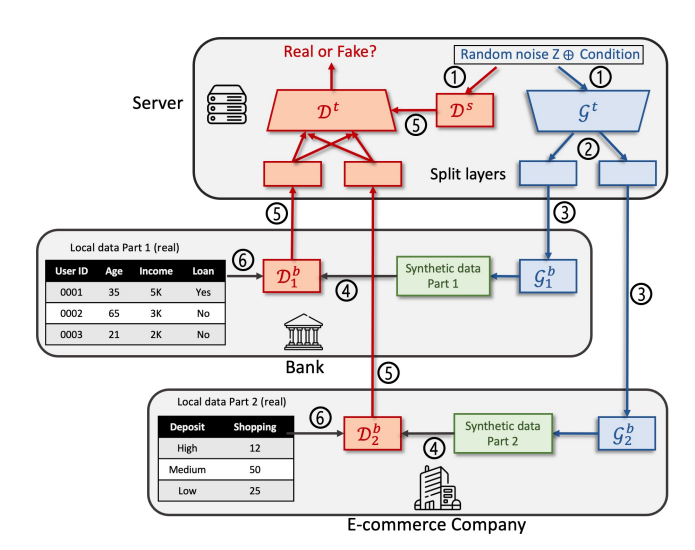


Figure 3: The workflow of VT-GAN.

introduce the threat model of our framework followed by a walkthrough of the training process. We then delve into the specifics of training, including possible adjustments. Secure design for publishing synthetic data is explained in the end.

3.1.1 VT-GAN overview. Fig. 3 shows an example of VT-GAN with two clients. The notions of the components are provided in Tab. 1. Each client contains unique data columns. VT-GAN establishes a separate server instead of assigning the client that holds the label as server, as in Fig. 1. The reason is twofold: (1) In table synthesis, when label column is not needed, no label holder exists. (2) For privacy reasons, clients should not access both the CVs and selected data indices. The server also should not have access to the shuffle function that the client uses to shuffle local data (we discuss this function in more detail in Section 3.1.4). In Fig. 3, one notable feature is the partition of the discriminator and generator between the server and the clients. The design of the bottom models, i.e., $\mathcal{D}_1^b, \mathcal{D}_2^b$ and $\mathcal{G}_1^b, \mathcal{G}_2^b$, are also motivated by privacy concerns. First, \mathcal{D}_1^b and \mathcal{D}_2^b are used because clients cannot directly send their real data to the server. Second, \mathcal{G}_1^b and \mathcal{G}_2^b are necessary because otherwise, the output from \mathcal{G}^t would only go through \mathcal{D}_1^b , \mathcal{D}_2^b and return to the server. If so, the server could reverse-engineer \mathcal{D}_1^b , \mathcal{D}_2^b and reconstruct the clients' data. One may also question the necessity of \mathcal{D}^t and \mathcal{G}^t . Without \mathcal{D}^t , all generations would be examined only by discriminators in each client. As a result, the generations from different clients would not be correlated because their correlations are never checked. Similarly, without \mathcal{G}^t , each client would sample a separate random noise vector for $\mathcal{G}^b_{\scriptscriptstyle 1}$ and \mathcal{G}_2^b , which would prevent the synthetic data from learning column correlations across clients since there is no correlation between two separate random noise vectors.

3.1.2 Threat Model. In line with many previous works in the field of VFL [12, 16, 17, 49], we focus on the semi-honest model in the design of our proposed VT-GAN architecture. Specifically, we assume that the clients and server are honest but curious, and their behaviors obey the following rules:

Algorithm 1: VT-GAN Training Process

```
Input: Number of client N; Server side generator G^t and
                 discriminator \mathcal{D}^t; Conditional vector filter \mathcal{D}^s;
                 Client side generator \mathcal{G}_{i}^{b}, discriminator \mathcal{D}_{i}^{b} and data
                 T_i for client i, i \in [1, N]; Training round R.
                 Discriminator training epochs per round e.
    Output: Trained Generator \{\mathcal{G}^t, \mathcal{G}_i^b\}, Discriminator \{\mathcal{D}^t, \mathcal{G}_i^b\}
                     \mathcal{D}^{s}, \mathcal{D}_{i}^{b}
    Client i (i \in [1, N]) operates:
 1 Encode(T_i);
 <sup>2</sup> while current round < R do
           Train Discriminator, freeze \{\mathcal{G}^t, \mathcal{G}_i^b\}:
           while current local epoch < e do
                  Server operates:
                  CV_p, idx_p < - CVGeneration(N clients) where the
  4
                    condition column is constructed by Client p
                  \{\mathcal{G}_{i}^{t}(Z,CV_{p}),i\in[1,N]\}\ <- Split(\mathcal{G}^{t}(Z,CV_{p}))
  5
                  Client i (i \in [1, N]) operates:
                 Output \mathcal{D}_i^b(\mathcal{G}_i^b(\mathcal{G}_i^t(Z,CV_p))) as \mathcal{D}_{out}^{b,i} to server; Server operates:
                  \mathcal{D}_{inS}^{t} \leftarrow \text{Concat}(\mathcal{D}_{out}^{b,i}, \mathcal{D}^{s}(CV_{p})), i \in [1, N]);
                 Output \mathcal{D}^t(\mathcal{D}_{inS}^t);
 8
                  Client i (i \in [1, N]) operates:
                 if i == p then
                        Output \mathcal{D}_p^b(T_p[idx_p]) to server;
 10
11
                        Output \mathcal{D}_i^b(T_i) to server;
 12
13
                  end
                  Server operates:
                  \begin{split} \mathcal{D}_{inR}^t &\leftarrow \mathsf{Concat}(\mathcal{D}_i^b(T_i)[idx_p], \, \mathcal{D}_p^b(T_p[idx_p]), \\ \mathcal{D}^s(CV_p)), \, i \in [1,N] \text{ and } i \, ! = p); \end{split} 
14
                 Output \mathcal{D}^t(\mathcal{D}^t_{inR}); Calculate Loss \mathcal{D}(\mathcal{D}^t(\mathcal{D}^t_{inS}), \mathcal{D}^t(\mathcal{D}^t_{inR})) and
15
16
                    update \{\mathcal{D}^t, \mathcal{D}^s, \mathcal{D}_i^b\}.
           end
           Train Generator, freeze \{\mathcal{D}^t, \mathcal{D}^s, \mathcal{D}_i^b\}
           Server operates:
           CV_p, idx_p < - CVGeneration(N clients) where the
18
             condition column is constructed by Client p
           \{\mathcal{G}_{i}^{t}(Z,CV_{p}),i\in[1,N]\}\ <- Split(\mathcal{G}^{t}(Z,CV_{p}))
19
           Client i \ (\hat{i} \in [1, N]) operates:
           Output \mathcal{D}_{i}^{b}(\mathcal{G}_{i}^{b}(\mathcal{G}_{i}^{t}(Z,CV_{p}))) as \mathcal{D}_{out}^{b,i} to server;
20
           Server operates:
           Server operates. \mathcal{D}_{inS}^{t} < -\operatorname{Concat}(\mathcal{D}_{out}^{b,i}, \mathcal{D}^{s}(CV_{p})), i \in [1, N]); Calculate \operatorname{Loss}^{\mathcal{G}}(\mathcal{D}^{t}(\mathcal{D}_{inS}^{t})) and update \{\mathcal{G}^{t}, \mathcal{G}_{i}^{b}\};
21
           Client i (i \in [1, N]) operates:
           Shuffle(T_i), i \in [1, N];
23
24 end
```

 All clients and the server comply with the VT-GAN protocol and execute the training process honestly.

- (2) While any client or server may attempt to extract additional information from the exchanged messages, none of them intentionally modify the values to disrupt the VT-GAN training process.
- (3) Clients do not engage in any collusion to exchange information with other clients or the server except for necessary messages.

These assumptions form our threat model for the VT-GAN architecture, and our design aims to address potential threats that may arise under these assumptions.

3.1.3 VT-GAN Training Procedure. The training process of VT-GAN is similar to that of a centralized tabular GAN, despite the fact that VT-GAN distributes the default tabular GAN into multiple separate components. As the example shown in Fig. 3, the workflow is numerated, parallel actions are noted with the same numbers.

During the discriminator training phase, the process starts with the generator. After initializing the random noise and conditional vectors, they are concatenated and fed to \mathcal{G}^t and \mathcal{D}^s (i.e., 1). The data is then passed through 2 to 5. After 5, the server concatenates the intermediate logits and uses the concatenation as input for \mathcal{D}^t to produce predictions for the synthetic data. At the same time, clients select their real training data following 6 then 5, and the server concatenates the intermediate logits and produces predictions for the real data. These predictions for real and synthetic data are used to calculate the gradients for updating $\{\mathcal{D}^t, \mathcal{D}^s, \mathcal{D}^b_1, \mathcal{D}^b_2\}$.

During the generator training phase, the process also begins with the generator. The concatenation of the random noise and conditional vectors is passed through ① to ⑤, and \mathcal{D}^t produces predictions. These predictions are used to update $\{\mathcal{G}^t, \mathcal{G}_1^b, \mathcal{G}_2^b\}$. Once all network components are updated, one training round is complete. At the end of each training round, all clients shuffle their local training data using the same random seed to ensure data consistency between them.

3.1.4 Training Details. Algo. 1 elaborates the training flow detail. The whole process involves of several functions, namely Encode, CVGeneration, Split, Concat, Loss $^{\mathcal{D}}$, Loss $^{\mathcal{G}}$ and Shuffle. In step 1, each client needs to encode their local data. One-hot encoding for categorical column, mode-specific normalization [51] for categorical column and mixted-type encoder [55] for column contains both categorical and continuous values. In step 3, the training of discriminator needs a local training epochs e because our tabular GAN algorithm is based on Wasserstain GAN plus gradient penalty [21] loss function. This training method needs more discriminator update (by default e = 5) than generator; In step 4, server uses CVGeneration to notify all the clients to generate their local conditional vector (CV) based on the CV construction method proposed by CT-GAN [51], then it randomly choose one of the clients' CVs based on the probability vector P_r calculated by the ratio of number of features in the client to the total number of features across all the clients. The selected client p does not only upload the CV_p to the server, but also the indices of selected training data idx_p that meets the conditions represented in CV_p . Due to privacy concern, the idx_p is only kept between the selected client and server, and the potential risk is discussed in Sec. 3.1.6. In step 5, Split function vertically splits output logits proportionally

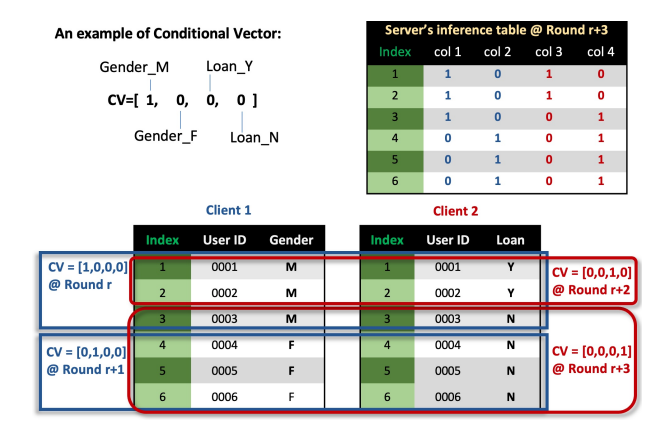


Figure 4: VT-GAN training without shuffling.

based on the ratio vector P_r . In step 7, Concat function horizontally concatenates all the intermediate logits into one input \mathcal{D}^t_{inS} . During step 9 to 13, for the client p, it just needs to select out the idx_p training data and passes through the $\mathcal{D}^b_p(T_p[idx_p])$. For the rest of the clients, they need to pass all their local data through the local discriminator; Then in step 14, except the output from client p, the server needs to first use idx_p to select their outputs, then concatenate all these intermediate logits into one input \mathcal{D}^t_{inR} . In step 16, With \mathcal{D}^t_{inS} and \mathcal{D}^t_{inR} , we can use Loss \mathcal{D} to calculate gradients and update all discriminator parts. The training steps for the generator from 18 to 21 are the same as the steps from 4 to 7. The difference is that to update the generator, function Loss \mathcal{G} (i.e., the step 22) only needs \mathcal{D}^t_{inS} .

3.1.5 Training-with-shuffling. At the end of each training round (i.e., step 23 in Algo. 1), we need to call Shuffle on all the clients in order to shuffle their local training data. Moreover, all the clients share the same random seed inside their Shuffle function, which means after Shuffle, each data row across all the clients is still aligned to the same ID, only the data index changes. We assume that Shuffle function and random seed are securely negotiated among all the clients before training and isolated from server.

Fig. 4 shows an example of VT-GAN training WITHOUT Shuffle in step 23 in Algo. 1. Assuming the system contains two clients and each client contains only one feature, i.e., Gender and Loan, respectively. Both features are categorical columns and each of them has only two classes. According to the CV construction method of CT-GAN, the CV of our example contains four bits, each of which represents one class of the categorical columns, and we can only indicate one class per CV. For each training round, we sample new CVs, and the corresponding classes of selected local training data need to match the new CVs. For example, at round r, if our sampled CVs contain three [1,0,0,0] vectors, then the corresponding data indices (1,2,3) also return to the server (i.e., step 4 in Algo. 1), then round r + 1 with three [0,1,0,0] in CVs and indices (4,5,6), round r + 2 with two [0,0,1,0] in CVs and indices (1,2), and finally round r + 3 with four [0,0,0,1] in CVs and indices (3,4,5,6). The server can use the indices and CVs obtained during the training process to reconstruct the entire dataset after a certain number of rounds, as illustrated in Figure 4. Despite not having knowledge of the number of categorical columns or their names in the system, the server can

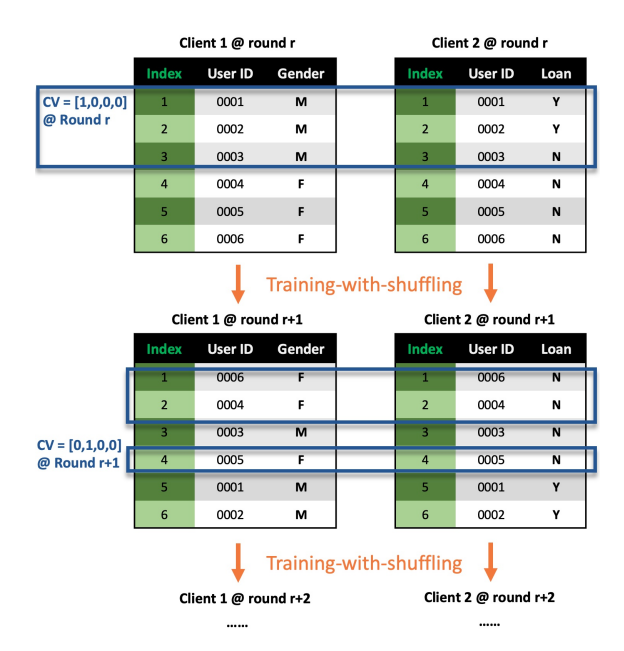


Figure 5: VT-GAN training-with-shuffling.

infer this information by analyzing the one-hot encoding of each row. In Figure 4, after round r+3, the server can deduce that there are two categorical columns in the system, each containing two categories. Additionally, the server can infer the ratio of categories within each column, such as a 1:1 ratio for the first column and a 1:2 ratio for the second column. If the synthetic data is released by clients, the server can determine the corresponding column names by analyzing the ratio of categories in all categorical columns.

Fig. 5 shows an example of the VT-GAN with *training-with-shuffling*. At round r, we still sample CVs that contain three [1,0,0,0] vectors and get the corresponding data indices (1,2,3). But this time, we launch the shuffling function in each client. At round r+1, we can see that the index column remains the same as last round but the data content part have shuffled, and more important the client 1 and client 2 have the same order in User ID column. If round r+1 sampled CVs that contains three [0,1,0,0], the server gets the indices [1,2,4]. But these indices in the new round corresponds to different data content. Therefore, the server cannot reconstruct clients' data.

3.1.6 Further Discussion. Incorporating CV into the training of the VT-GAN algorithm is not a straightforward task. Since CV is a part of the generator's input, it cannot be hidden from the server. However, we have control over whether to pass selected data indices to the server. VT-GAN chooses to share this information with the server, so at step 12, we allow clients who do not contribute CV to pass their entire local data through \mathcal{D}_i^b , and then at step 14, the server selects the corresponding indices data from the intermediate logits. This design increases local computation and communication between the server and clients, but it ensures that there is no privacy leakage. In order to decrease the overall training time, certain calculations can be performed in parallel. After step 4, all the clients are aware of whether their conditional vectors have been selected. Therefore, all the clients are able to execute steps 10 or 12 right after step 4.

An alternative approach to design VT-GAN is to make clients share the selected data indices in a peer-to-peer (P2P) manner rather than with the server. In this case, the server would not have access to the indices information, and clients would only need to pass the selected data rows through local \mathcal{D}_{i}^{b} . However, this solution has several limitations. Firstly, maintaining P2P connections among all the clients can be costly and insecure, as the number of connections increases exponentially with the number of clients. Additionally, this approach also indirectly leaks clients' privacy. To balance the class imbalances in the columns of real data, the CV of CT-GAN is sampled based on the log-frequency of class appearances in the column. As a result, there may be scenarios where several data rows containing the minority class are selected multiple times in one training epoch, often together. In this case, a client who does not contribute CV in the current training round could reasonably infer that the data in these indices have common features in a certain column of the CV contributor, which causes a privacy leakage. Adding shuffling to this design cannot solve above inference. Because in VFL, we can only shuffle the index of data, the mapping of other features among all clients remain the same (see Fig. 5), all the clients can observe the repeated selected group of data if it exits.

3.1.7 Synthetic Data Publication. Once the training is complete, the secure publication of synthetic data becomes a crucial step in the VT-GAN framework. In practical scenarios, the server receives a request for a specific amount of synthetic tabular data and responds by sending an equivalent amount of random noise to the generator \mathcal{G} . The clients independently use their own generators \mathcal{G}_i^b to generate their respective synthetic data portions, which are then concatenated to form the final synthetic dataset.

To ensure privacy preservation, clients must shuffle their synthetic data before publication. Without shuffling, the server would have partial black-box access [6] to \mathcal{G} , which assumes knowledge of the inputs (random noise) and outputs (published synthetic data), including the input-output pairs. This partial black-box access poses significant privacy risks in VT-GAN, enabling independent attacks by the server without client collusion. Hence, shuffling before publishing is essential to eliminate partial black-box access, preventing the server from possessing knowledge of the input-output pairs of \mathcal{G} . It is important to note that in VT-GAN, nothing beyond the final synthetic data is published. The partial neural networks employed by the clients and server are considered private assets and are not deployed as part of the API.

3.2 Privacy Analysis in VT-GAN Training Flow

According to threat model, here we analyze the privacy leakage risk in VT-GAN training, and explain the motivations behind our design. We highlight the sensitive information exchanged and used in VT-GAN, including feedforward activations, and backpropagation process on $\mathcal G$ and $\mathcal D$, model weights, and model gradients. Here both $\mathcal G$ and $\mathcal D$ represent the combination of top and bottom generator and discriminator in VT-GAN.

Feedforward in Generator. The input data of this process is a combination of random noise Z and conditional vector CV, which is passed through the neural network layers of \mathcal{G} until it reaches the output layer on each client. Finally, the corresponding piece of synthetic tabular data is generated on each client as the

output. Obviously, none of the participants is able to reconstruct real records during this process since the real tabular datasets T_i are not used throughout this process. Even if all clients except one collude with the server to infer information about the remaining client, the inferred information is only about synthetic data, which is actually intended to be published in our design.

Backpropagation in Generator. In this process the generator \mathcal{G} takes the loss $\mathsf{Loss}^{\mathcal{G}}(\mathcal{D}^t(\mathcal{D}^t_{inS}))$ as input and updates its model parameters using the Stochastic Gradient Descent (SGD) method. Leakage of labels is a significant concern in the backpropagation process of traditional VFL classification models[14, 17]. However, this risk does not apply for \mathcal{G} because (i) the backpropagation of \mathcal{G} does not involve the use of real dataset T_i , as outlined in Section 3.1.4; (ii) \mathcal{G} is not a classifier, and thus, the concept of 'label' is not applicable. It is possible for the client to infer the CV by examining changes in gradients[14]. Nonetheless, as elaborated in Section 3.1.5, only the selected client knows which rows are selected based on its CV. Neither server nor other clients can reconstruct selected client's data only by CV. Therefore, the leakage of CV is not considered as a significant privacy risk.

Feedforward in Discriminator. The architecture of discriminator \mathcal{D} aligns more closely to a traditional VFL classifier. The main difference lies in the labels of the training data. In the training process of a VFL classifier, the label column is held by one of the clients, who also manages the server, as illustrated in Fig. 1. In VT-GAN, the labels for training \mathcal{D} are only real and fake, which are not part of the original tabular dataset. Additionally, it is each client who labels real and fake for the data instances. Therefore, the threat models mentioned in [14, 17, 31] do not apply for \mathcal{D} , since they all assume that a malicious client, or multiple clients, attempt to infer the label column which they do not possess.

The intermediate logits sent from clients to the server may contain sensitive information about the dataset. An example of this is mentioned in [17], which points out that the server can determine if two records have the same categorical values by comparing their intermediate logits during the feedforward process. VT-GAN mitigates the risk like that because the server is independent from all the clients and it does not hold any information about the dataset.

Backpropagation in Discriminator. As mentioned above, the clients already know the *real* and *fake* labels of the training data prior to the training of \mathcal{D} , thus the label leakage problem [17] of the backpropagation process is not an issue in VT-GAN. One potential risk is that malicious clients may collude with the server to infer sensitive information about the training data of the victim client. However, it is important to note that this information, such as distributions and imbalanced features, is an inherent aspect of the final product of VT-GAN, which is a joint synthetic tabular dataset. Therefore, it can be argued that this risk is justified in the application scenario of VT-GAN, as clients who participate in the program are aware of such risks.

Model weights and model gradients. The model weights are considered intensive information in VFL studies [17, 49], since the values indicate the relative importance of each feature for the learning tasks. In VT-GAN, this may cause feature importance leakage once the malicious clients share the trained model weights of $\mathcal D$ with the server. As mentioned above, the feature importance here is

only in reference to the impact of the features on distinguishing real and synthetic data. Additionally, while traditional VFL tasks take the trained model as the final product and it is normal to share the model weights among clients, our VT-GAN sees the joint synthetic dataset as the ultimate outcome. As a result, model weights are supposed to be kept safe and never exposed in VT-GAN.

Recent studies [18, 28, 57] have shown that model gradients can lead to privacy leakage. In [28], the authors present a new algorithm CAFE for recovering large amounts of private data from shared aggregated gradients in the VFL settings. CAFE has a high recovery quality and is backed by theoretical guarantees. However, the assumptions made by the algorithm are quite restrictive and may not be practical for our VT-GAN scenarios. One of the key prerequisites in [28] is that the server knows the data index, which is not feasible in our settings. Just as with the privacy of model weights, the risk of data leakage from gradients can only occur when malicious clients are working in collusion with the server.

In summary, when malicious participants act alone, the VT-GAN system is robust to privacy leakage issues present in traditional VFL. However, the system becomes vulnerable when multiple parties collude. This can lead to even more severe security problems, as other advanced attacks may also pose a threat to VT-GAN. These issues are discussed in greater detail in the following section.

3.3 Security Analysis

Here, we discuss the adversarial attacks in the context of VT-GAN. Feature inference attack. For the feature inference attacks in VFL, Luo et al. [36] first propose attacks on the logistic regression (LR) and decision tree (DT) models and achieve high attack accuracy. However, these attacks are not applicable to complex models such as neural networks. In our VT-GAN architecture, both $\mathcal G$ and \mathcal{D} are neural network models characterized by the presence of multiple hidden layers that facilitate non-linear transformations. This structure poses a natural barrier to equality-solving attacks based on solving equations and the maximum a posteriori (MAP) method [13]. Luo et al. [36] then design a generative regression network (GRN) to learn the correlations between the malicious client's and victim client's features. Even for complex neural network models, GRN manages to infer the distribution of feature values with high accuracy. However, this method relies on the assumption that the trained VFL model is given to the attacker. As discussed in the previous section, although publishing the trained models is the common case in VFL scenarios, it is prohibited in VT-GAN. In other words, conducting [36]'s feature inference attack on VT-GAN requires the attacker to steal model parameters of \mathcal{G} and \mathcal{D} from all participants, which is unrealistic.

Label inference attack. Label leakage problem has been widely studied for VFL [14, 31, 47]. Although the results show that the malicious client succeeds to infer some label information, these studies are case-specific and have some limitations. [31] works only for the case of binary classification model training between two VFL clients. [14] is based on the assumption that the adversary has a small amount of auxiliary labelled data to fine-tune the attack model. Moreover, as discussed in Section 3.2, the *real* and *fake* label in VT-GAN is not part of the tabular original dataset and is managed by

clients. To the best of our knowledge, such label inferences attacks on VT-GAN do not make much sense as in traditional VFL cases.

Membership Inference Attack. In addition to the aforementioned privacy threats on VFL, a distinct form of attack, known as the Membership Inference Attack (MIA), specifically targets generative models such as GANs [6, 24, 26]. The MIA is executed in the following manner: the adversary is granted access to the machine learning model, which could be black-box or white-box access depending on the specific scenario. The adversary also has access to a set of data records. By conducting MIA, the adversary attempts to infer whether a data record has been used to train the model. This could potentially expose sensitive information.

In the structure of VT-GAN, the generator $\mathcal G$ is partitioned into top and bottom models, each owned by separate participants. Consequently, it appears implausible to posit that an attacker can gain white-box access to the entire $\mathcal G$, as this presumes a full collusion between all clients and the server. As discussed in Section 3.1.7, the shuffling mechanism prior to publishing mitigates partial black-box access to $\mathcal G$. Nonetheless, under our threat model, the possibility remains for an adversary to conduct MIA with full black-box access, which means the attacker is only permitted to access the generated samples set from the well-trained black-box $\mathcal G$. In Section 4.3.4, we execute [6]'s full black-box MIA on VT-GAN, thereby assessing the effectiveness of the privacy protection measure - Differential Privacy (DP), in counteracting this attack.

4 EMPIRICAL EVALUATION

4.1 Experiment Setup

Datasets Our algorithm is tested on five commonly used machine learning datasets: Adult, Covertype, Intrusion, Credit, and Loan. Adult, Covertype, and Intrusion are obtained from the UCI machine learning repository*, while Credit and Loan are obtained from Kaggle*. All five datasets contain a target variable. Although it is not required for a tabular dataset to have a target column for data synthesis, we have chosen to use datasets with a target column for the purpose of classification evaluation. This allows us to test the utility of the synthetic data for machine learning tasks compared to real data. Due to computing resource limitations, we randomly sample 50K rows of data in a stratified manner with respect to the target variable for the Covertype, Credit, and Intrusion datasets. The Adult and Loan datasets are not sampled. For all the datasets, we train the algorithms 300 epochs for all the experiments. Each experiment is repeated three times and the average result is reported.

Baseline To the best of our knowledge, VT-GAN is the first architecture to incorporate SOTA tabular GAN into vertical federated learning. Our baseline for comparison is therefore a **centralized tabular GAN**. To have a better centralized baseline, we have adopted various techniques from CT-GAN [51] and CTAB-GAN [55]. These include the use of one-hot encoding for categorical columns, mode-specific normalization for continuous columns, mixed-type encoder for columns containing both categorical and continuous values. The construction method of the conditional vector is also adopted from CT-GAN. All of these techniques are incorporated into our centralized tabular GAN. The generator and

^{*}http://archive.ics.uci.edu/ml/datasets

^{*}https://www.kaggle.com

discriminator structures are the same as in CT-GAN. The generator is a Resnet-style [22] neural network comprising two residual blocks followed by a fully-connected (FC) layer. Each residual network (RN) block includes three successive layers: FC, batchnorm, and relu. The discriminator has two fully-connected network (FN) blocks followed by another FC layer. Each FN block consists of three successive layers: FC, leakyrelu, and dropout. The output dimension for all the RN block and FN block is fixed to 256.

Testbed The experiments are conducted on two machines running Ubuntu 20.04. Both machines are equipped with 32 GB of memory, an NVIDIA GeForce RTX 2080 Ti GPU, and a 10-core Intel i9 CPU. One machine serves as the server, while the other hosts all the clients range, with the number of clients ranging from 2 to 5.

4.2 Evaluation Metrics

We evaluate the synthetic data in two dimensions: (1) **Machine Learning (ML) Utility** and (2) **Statistical Similarity**. The two dimensions cover the row-wise correlation and column-wise distribution of the synthetic data. Given the local training data RD_A and RD_B for clients A and B, respectively, the synthetic data produced by the clients is denoted as SD_A and SD_B . Unless otherwise stated, in the following context, synthetic data refers to the concatenation of SD_A and SD_B , and real data refers to the concatenation of RD_A and RD_B .

4.2.1 Machine Learning Utility. To evaluate the effectiveness of synthetic data for machine learning tasks, we have designed the following evaluation pipeline. We first split the original dataset into training and test sets. The training set (i.e., RD_A and RD_B) is used as input to the VT-GAN models to generate synthetic data of the same size. The synthetic and real training data are then used to train five widely used machine learning algorithms (decision tree classifier, linear support vector machine, random forest classifier, multinomial logistic regression, and multi-layer perceptron). The trained models are then evaluated on the real test set. Performance is measured using accuracy, F1-score, and the area under the curve (AUC) of the receiver operating characteristic curve, difference between models trained by real and synthetic data is reported. The goal of this design is to determine whether synthetic data can be used as a substitute for real data to train machine learning models.

4.2.2 Statistical Similarity. Three metrics are used to quantify the statistical similarity distance between real and synthetic data.

Average Jensen-Shannon divergence (JSD). The JSD is a measure of the difference between the probability mass distributions of individual categorical columns in the real and synthetic datasets. It is bounded between 0 and 1 and is symmetric, making it easy to interpret. We average the JSDs from all the categorical columns to obtain a compact, comprehensible score.

Average Wasserstein distance (WD). We find that the JSD metric is numerically unstable for evaluating the quality of continuous columns, especially when there is no overlap between the synthetic and original datasets, so we chose to use the more stable Wasserstein distance to measure the similarity between the distributions of continuous/mixed columns in synthetic and real datasets. We average all column WD scores to obtain the final score.

Difference in pair-wise correlation (Diff. Corr.). To evaluate the preservation of feature interactions in synthetic datasets, we compute the pair-wise correlation matrix separately for real and synthetic datasets. The dython library is used to compute correlation matrix for each table. The l^2 -norm of difference between the real and synthetic correlation matrices is then calculated and abbreviated as Diff. Corr.. In the neural network partition experiment with two clients, to examine the preservation of column correlations within each client and between two clients, we first separately calculate the **Diff. Corr.** for each client's data, and then name the average results **Avg-client**, we also report the difference of correlation matrices between both clients' data, the result is named Across-client. Assuming clients A and B, with their local real data RD_A and RD_B , respectively, produce synthetic data SD_A and SD_B . Avg-client averages the **Diff. Corr.** of $\{RD_A, SD_A\}$ and **Diff. Corr.** of $\{RD_B, SD_B\}$. Across-client calculates the l^2 -norm of difference between the correlation matrix of $\{RD_A, RD_B\}$ (i.e., pair-wise correlation between columns in RD_A and RD_B) and the correlation matrix of $\{SD_A, SD_B\}$. These two metrics are designed to demonstrate the ability of VT-GAN to capture intra- and interdependencies of training data columns within and across clients.

4.3 Result Analysis

The goal of the experiments is to determine the optimal configuration of VT-GAN for synthesizing high-fidelity tabular data. To this end, we aim to answer three research questions: (1) What is the optimal partition of generator and discriminator neural networks between the server and clients? (2) How does VT-GAN respond to variations in number of data features across clients. (3) How does VT-GAN adapt to changes in the number of clients participating in the system. To answer these questions, we have designed three experiments. The centralized baseline serves as the basic tabular GAN algorithm for VT-GAN to distribute and train in VFL. In practice, the number of clients in a VFL scenario is constrained by the number of features in the tabular dataset. Therefore, following the VFL experiments setup in [14, 17, 36], our first two experiments are performed in a two-client setting. The VT-GAN architecture can be readily expanded to accommodate more clients. We assess the influence of the number of clients in Section 4.3.3.

4.3.1 Neural Network Partition. For this experiment, we evenly split the training datasets for two clients (or one client may have one more column if the total number of columns is odd), and the column orders are preserved as they were downloaded. As illustrated in Fig. 6, we propose three ways to partition the neural networks of both the generator and discriminator across the server and clients. Both the generator and discriminator have two network blocks (same as in centralized baseline), so we consider three divisions for each of them: (i) all blocks in the server, (ii) one block in the server and one block in each client, (iii) all blocks in the client. This results in a total of nine combinations. The partition notions of $G_{n_2}^{n_1}$ and $D_{n_3}^{n_3}$ are explained in Fig. 6. The sum of the output dimension of partitioned RN/FN block is the same as in their centralized scenario, i.e., 256. The output dimension of each partitioned block is calculated based on the ratio vector P_r for each client.

^{*}http://shakedzy.xyz/dython/modules/nominal/#compute_associations

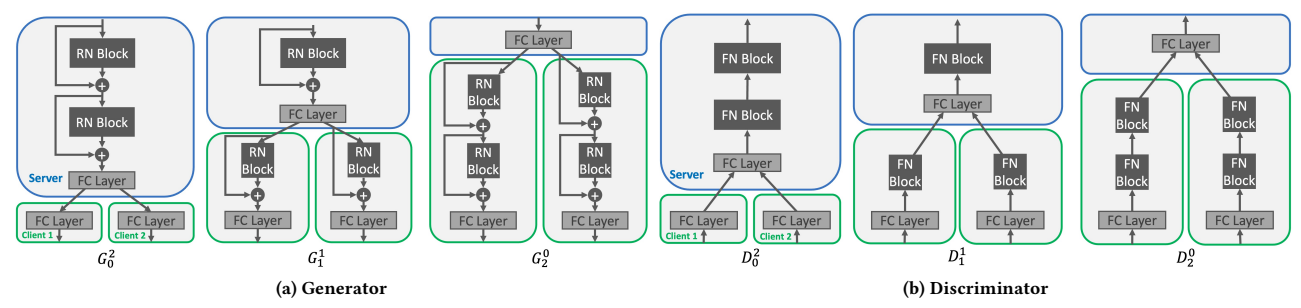


Figure 6: Neural Network Partition. $G_{n_2}^{n_1}$ denotes the generator with n_1 RN block(s) in server and n_2 RN block(s) in each client. $D_{n_4}^{n_3}$ denotes the discriminator with n_3 FN block(s) in server and n_4 FN block(s) in each client.

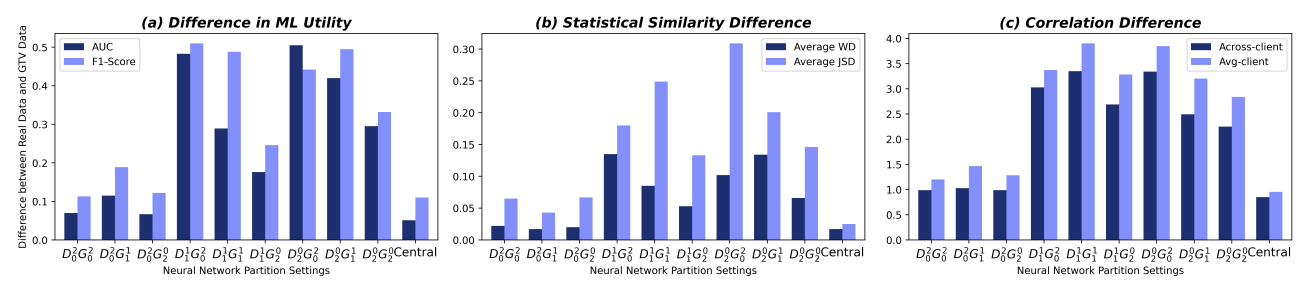


Figure 7: Neural network partition results: the difference between real and VT-GAN data. A lower value indicates higher quality.

Figure 7 shows the neural network partition results where all results are averaged over five datasets. In all three subfigures, it is clear that the centralized method performs best on all metrics, as expected. Of the other partition methods, $D_0^2G_0^2$, $D_0^2G_1^1$, and $D_0^2G_2^0$ stand out as they consistently outperform the other six configurations on all metrics. These three partition methods have all the FN blocks on the server side. Among these three, $D_0^2G_1^1$ performs slightly better in terms of statistical similarity and slightly worse in correlation difference, but clearly worse in terms of ML utility compared to the other two. $D_0^2G_0^2$ and $D_0^2G_2^0$ show similar results across all evaluation metrics and consistently outperform all other configurations in terms of ML utility. $D_0^2G_0^2$ achieves F1-score only 2.7% lower to the centralized method. Above result suggests that having a sufficiently large discriminator on the server side is crucial to the success of VT-GAN, and that VT-GAN can achieve performance similar to the centralized method if the discriminator and generator are properly positioned.

Based on the overall performance, we consider $D_0^2G_0^2$ and $D_0^2G_0^2$ to be the two best configurations for VT-GAN. To choose between these two configurations, we must consider the computation and communication overhead of the system. In terms of communication overhead, their only difference is the size of the intermediate logits transferred between the server and clients for generator, which can be controlled by the FC layer before logits are sent from the server to the client. In current setting, $D_0^2G_0^2$ has higher communication overhead; In terms of computation overhead, if the server is powerful, placing both the generator and discriminator on the server can speed up the training process. However, many computations are now performed on the cloud, there is a cost associated with using the server. It may be more cost-effective to distribute calculations to the clients. Additionally, as the number of clients increases, the

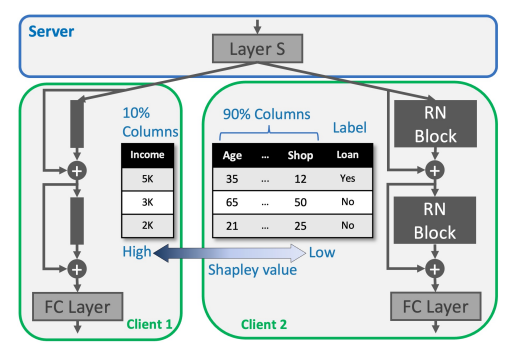


Figure 8: An example of the G_2^0 generator partition in 1090 data partition experiment.

generator can become larger, making it more expensive to place the entire generator on the server side. Therefore, when $D_0^2G_0^2$ and $D_0^2G_0^2$ achieve the similar result, $D_0^2G_0^2$ is preferred.

4.3.2 Training Data Partition. Experiment in Sec. 4.3.1 suggests that $D_0^2G_0^2$ and $D_0^2G_2^0$ are two optimal configurations for VT-GAN when data features are randomly and evenly distributed among two clients. In this experiment, we examine the impact of data partition on these setups of VT-GAN. For each dataset, we use the Shapley value [35] to evaluate the importance of each feature in predicting the target column using a MLP (Multi-layer Perceptron) model with one hidden layer containing 100 neurons. We sort the features importance and consider three different feature divisions: (i) 1090: the 10% most important features and the remaining 90%, (ii) 5050: 50% most important features and 50% remaining features, and (iii) 9010: 90% most important features and 10% remaining features. For each division, we assign the two parts to two clients. The target column is always located on the client WITHOUT the most important

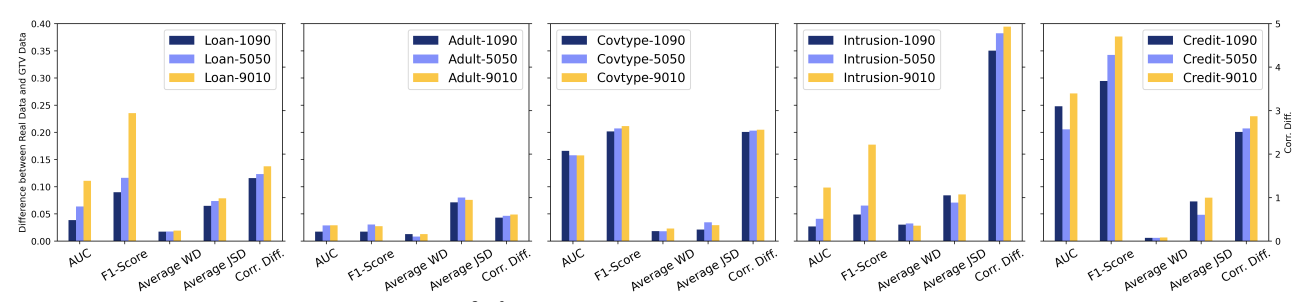


Figure 9: Data partition results with $D_0^2G_2^0$: the difference between real and VT-GAN data. Corr.Diff. (right axis).

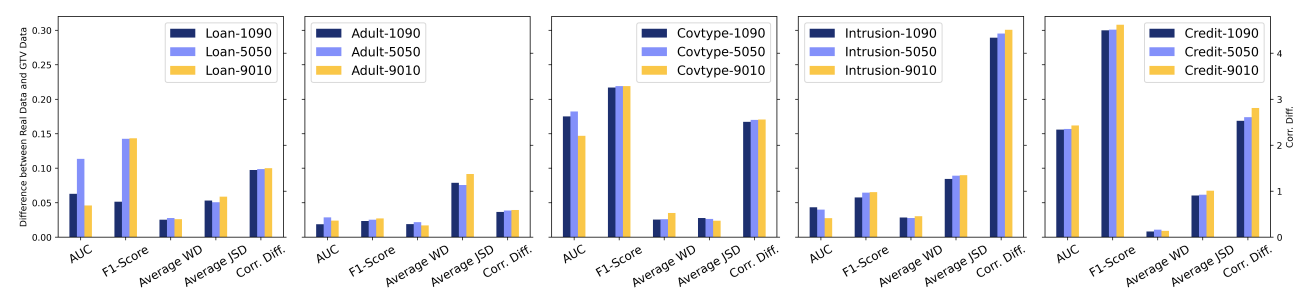


Figure 10: Data partition results with $D_0^2G_0^2$: the difference between real and VT-GAN data. Corr.Diff. (right axis)

features. The intuition behind these designs is that it is easier to learn the correlations among features within a single client than it is to learn correlations among features distributed across multiple clients. Fig. 8 shows an example 1090 data partition for G_2^0 . It is worth noting that when partitioning the data, we also split the RN block proportionally among the clients based on the ratio vector P_r . But the sum of the output dimension of the partitioned block is still the same as the centralized baseline, i.e., 256.

Fig. 9 shows the results for $D_0^2G_2^0$ on five datasets. Focusing on the ML utility metrics, we see that data partition has a smaller impact on the final synthetic data for the Adult and Covtype datasets, but a much larger impact on the Loan, Intrusion, and Credit datasets, where the 9010 partition leads to significantly worse results compared to the other two configurations. Regardless of the size of the impact, we observe on almost all datasets that the 1090 partition consistently performs better than the 5050 partition, which in turn performs better than the 9010 partition. This because each dataset contains several important features for predicting the target column, and as these features are excluded step-by-step from the label holder, it reduces VT-GAN's ability to fully capture the correlations between these features and the label. The results for statistical similarity are similar across all datasets and configurations. The results of the Diff.Coff. align with the ML utility results, which is expected since the preservation of column correlations is inherently linked to ML utility.

The results for $D_0^2G_0^2$ on the five datasets are shown in Figure 10. In terms of ML utility, especially the F1-Score, the 1090 partition performs best on all datasets. The results on Loan dataset are still affected by the data partition, However, it is also clear that $D_0^2G_0^2$ is much less impacted compared to $D_0^2G_0^2$. The results for statistical similarity for $D_0^2G_0^2$ are similar to those for $D_0^2G_2^0$, with little impact from the different data partitions on VT-GAN's ability to recover the column-wise distribution in the synthetic data. The Diff. Corr.

shows that the 1090 partition still outperforms the other two configurations. But comparing to $D_0^2G_0^2$, $D_0^2G_0^2$ is less affected by data partition. The reason is that the larger generator on the server side is able to better capture the column correlations across clients.

Comparing the result of $D_0^2G_2^0$ and $D_0^2G_0^2$ in the data partition experiment provides additional information to help us choose between these two configurations. In neural network partition experiment, when features are evenly and randomly distributed to clients, $D_0^2G_2^0$ and $D_0^2G_0^2$ achieve similar result, leading us to prefer $D_0^2G_0^2$ due to its lower cost and better scalability. However, when the data partition is extremely imbalanced, especially when the label holder contains significantly fewer features than other clients, $D_0^2G_0^2$ becomes the preferred configuration. One possible solution to increase the performance of $D_0^2G_0^2$ is to increase the size of neural network on the client who contains fewer features, this left for future work.

One might argue that when organizing a vertical federated learning group, the data partition is fixed and determined by the clients. However, when clients join vertical federated learning, it is possible for different clients to have overlapping features, and in such cases, we have the option to distribute more features to the label holder to improve ML utility for the synthetic data. This is because we only need one of the overlapping features to be present in the system. For datasets without a target column, we can try to balance the feature distribution among clients to avoid artificially creating imbalances that could degrade the training of VT-GAN.

4.3.3 Client Number Variation. For this experiment, we study the impact of number of clients on VT-GAN. We randomly and evenly distribute data columns into 2, 3, 4 and 5 clients on $D_0^2G_0^2$ and $D_0^2G_2^0$ configurations. For each dataset, the number of columns is fixed, the more clients in the system, the less data columns for each client. To address the potential performance degradation caused by an increasing number of clients in the system, we introduced two settings for the generator: (1) default and (2) enlarged. In the default

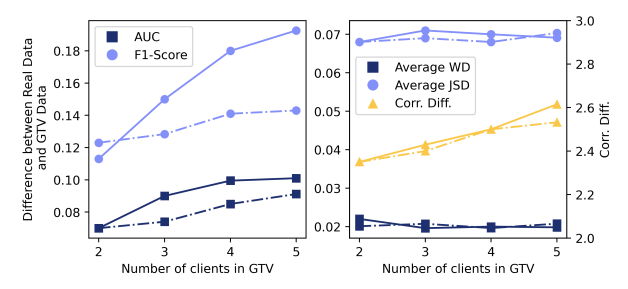


Figure 11: $D_0^2 G_0^2$ setting, the diff. between real and VT-GAN data over varied numbers of clients: default generator (firm line), enlarged generator (dashed line), Corr.Diff. (right axis).

setting, for $D_0^2G_2^0$, as the number of clients increases, we simply create more partitions of the original RN block. However, the sum of the output dimension of the divided RN block remains constant, at 256, as in the centralized case. The output dimension of all RN blocks is also 256 for $D_0^2G_0^2$. Default setting ensures, no matter how many clients join the system, the communication overhead between server and clients remains the same for $D_0^2G_0^2$ and $D_0^2G_0^2$, respectively; For the enlarged setting, we increase the output dimension of RN block to 768 (3 \times 256) for both $D_0^2G_0^2$ and $D_0^2G_2^0$, We will explain the reason for choosing this number with the results later.

Fig. 11 and 12 present the results on five metrics, with solid lines representing the results of the default setting and dashed lines representing the results of the enlarged setting. All results are averaged over five datasets. With default setting, the results show that with more clients in the system, i.e., each client contains less features, the ML utility of synthetic data becomes slightly worse. For example, as the number of clients increases from 2 to 5, $D_0^2G_0^2$ and $D_0^2G_2^0$ increase their F1-Score from 0.11 and 0.12 to 0.19, respectively; With enlarged setting, ML utility also decreases with increasing number of clients, but to a significantly lesser extent; The results of the Average WD and Average JSD indicate that the statistical similarity on both generator settings for both $D_0^2G_0^2$ and $D_0^2G_2^0$ remains largely unchanged regardless of the number of clients. Again, Coff.Diff. results are inline with ML utility. The result becomes worse with increasing number of clients for both settings. In most of scenarios, $D_0^2 G_2^0$ slight outperforms $D_0^2 G_0^2$

Therefore, in that case, $D_0^2 G_2^0$ is still the preferred configuration. The results for two settings on generator reveal that the *enlarged* setting has less variation as the number of clients increases. However, when there are only two clients in the system, the *enlarged* setting performs worse on the Loan dataset. The output dimension of the *enlarged* setting is determined through trial and error, highlighting the importance of considering the trade-off between the size of the neural network and the model convergence. It shows that increasing the size of the neural network does not always lead to improved results. Given that the Loan dataset only contains 5000 data instances, increasing the neural network size resulted in slower convergence for the generator in the *enlarged* setting. Optimal neural network size exploration for VT-GAN under different dataset and different number of clients is left for future work.

4.3.4 Membership Inference Attack on VT-GAN with Differential Privacy. As we discussed in Section 3.3, VT-GAN can be vulnerable to the full black-box MIA [6, 24, 26]. In our experiments, we conduct

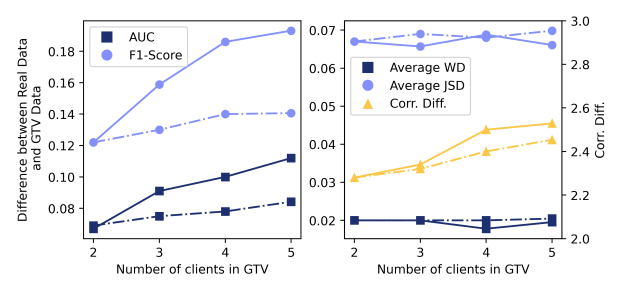


Figure 12: $D_0^2G_2^0$ setting, the diff. between real and VT-GAN data over varied numbers of clients: default generator (firm line), enlarged generator (dashed line), Corr.Diff. (right axis).

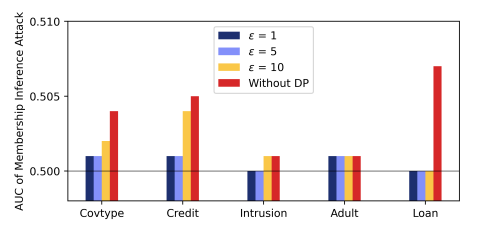


Figure 13: The result of Membership Inference Attack (full black-box) [6] on VT-GAN, under different DP settings.

[6]'s full black-box MIA on VT-GAN, and evaluate the performance of this attack on the five datasets. Moreover, we introduce Differential Privacy (DP) into VT-GAN as it is considered the most effective defense mechanism against MIA [5, 46, 50]. Specifically, we use the differential private (DP) stochastic gradient descent(SGD) [1] for training the discriminator (both client and server side) since only its training requires real data. The algorithm can be summarized into a two-step process. Firstly, the per-sample gradient computed during each training iteration is subject to clipping by its *L*2 norm using a predetermined threshold. Secondly, calibrated random noise is deliberately incorporated into the gradient to introduce stochasticity, thereby safeguarding privacy during the training process.

The results of the MIA conducted on all five datasets are presented in Fig. 13. In DP-SGD, the privacy budget ϵ determines the level of privacy protection. Smaller ϵ values offer stronger privacy guarantees but introduce larger amounts of noise into the model. It is evident that even without DP, the MIA is not highly effective, as a random guess model would achieve an AUC of 0.5. The AUC for the loan dataset is slightly higher than that for the other datasets because it contains fewer data records, which makes it more vulnerable to attack [6]. Nonetheless, despite the effect is weak, we observe that for the Covtype and Credit dataset, adopting DP reduces the AUC of the MIA.

DP affects the utility of model due to the addition of random noise during the training process. As for VT-GAN, we evaluate the impact of DP on the synthetic data quality. We conduct experiments on the $D_0^2G_0^2$ setting with random and evenly split features on two clients, same as setting in Sec. 4.3.1 where $D_0^2G_0^2$ performs among the best. We fix the privacy budget ϵ to three commonly used values (i.e., 1, 5, and 10 [25]) and compare the synthetic data quality with and without DP. Our results in Fig. 14, averaged over five datasets, indicate that DP significantly reduces the quality of the synthetic data in all metrics. Specifically, the average JSD and average WD between the original and synthetic data increase with DP. These

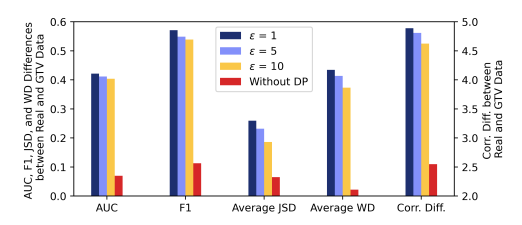


Figure 14: Under $D_0^2G_0^2 - 5050$ setting, The impact of Differential Privacy on VT-GAN performance. Corr.Diff. (right axis)

results suggest that it becomes more challenging to infer the original data distribution from the synthetic data. Increasing the privacy budget can enhance the synthetic data quality, but the improvement is still inadequate compared to the scenario without DP.

Take Aways The experiments show that a key factor for a successful VT-GAN is having a sufficiently large discriminator model on the server side. When the number of data columns is evenly distributed among two clients in VT-GAN, both $D_0^2G_2^0$ and $D_0^2 G_0^2$ exhibit similar performance and are comparable to the centralized algorithm. In cases where these two configurations yield comparable results, $D_0^2G_2^0$, i.e., distributes most of the generator network to client, is preferable due to its superior scalability and cost-effectiveness. However, when data is unevenly distributed among clients, then $D_0^2G_0^2$, i.e., distributes most of the generator network to server, is preferred. If control over the distribution of data columns among clients is possible, e.g., excluding certain overlapping data columns in certain clients, it is recommended to balance the number of columns among the clients in the system. With a fixed total number of features in the system, an increasing number of clients in VT-GAN reduces the quality of synthetic data. Strategically increasing the generator model size can effectively counter this performance degradation. For the security analysis, despite the limited effectiveness of DP in countering MIA, its adoption in VT-GAN significantly diminishes the quality of synthetic data, leading us to discourage the use of strong DP measures.

5 RELATED WORK

5.1 Vertical Federated Learning

While Horizontal Federated Learning (HFL) has been thoroughly studied [37, 52], Vertical Federated Learning (VFL) starts to gain more attention more recently [8, 15-17, 27, 34, 49]. Among them, [27] assumes that the label holder client's labels can be directly shared with others, which directly violates privacy. SecureBoost is proposed in [8] to use a lossless approach for training Gradient-Boosted Decision Trees (GBDT) in VFL scenario. VF²Boost [16] focuses on improving the efficiency of the GBDT algorithm under VFL setting by adopting a concurrent training protocol to reduce the idle periods. Liu et al. [34] achieve VFL Random Forest (RF) training based on the assumption of a third-party trusted server. In [49], the authors consider the use of Classification and Regression Trees (CART) in a VFL setting, which does not require the involvement of a third party but has the drawback of exponential complexity as the tree becomes deeper. Homomorphic Encryption (HE) and Secrete Sharing technologies are comprehensively applied in BlindFL [17] to protect VFL from most privacy attacks. An efficient VFL training framework with cached-enable local updates is proposed in [15] to

address the communication bottleneck across multiple participants. Li et al. [33] address the matrix factorization problem in VFL for training recommendation models. Though not designed for VFL, He et al. [23] propose TransNet to encrypt vertically partitioned data before sending it to the neural network, whereas the bottom model in VFL offers similar functionality. FedDA [53] trains separate GANs in each participant under VFL to achieve data augmentation. However, their study is centered on image generation, which is not a natural use case for VFL. Furthermore, their study does not incorporate the use of a conditional vector. VT-GAN trains only one GAN, adopts conditional vector, and supports multiple clients.

5.2 Privacy Preserving Techniques

Differential Privacy (DP)[11] has been extensively studied for GANs [5, 46, 50] and in HFL scenarios [19, 38, 41, 45] to provide provable privacy guarantees. In VFL with graph data processing, DP can be achieved by injecting noise into the sample representation [43]. Local Differential Privacy (LDP) has also been applied to VFL tree boosting models in a recent study [32]. However, there is currently no clear guidance on how to apply DP in VFL when dealing with both GANs and tabular data, i.e., the scenario of VT-GAN. Moreover, DP's utility is significantly limited due to the negative impact of noise injection on model performance, leading most VFL studies to deprecate its use [16, 17, 23, 34, 49, 53]. Another solution to enhance privacy in VT-GAN is through the use of multi-party computation (MPC) techniques including homomorphic encryption (HE) and secret sharing (SS) [17, 23, 34, 39]. BlindFL[17] presents the federated source layer based on the HE and SS techniques to achieve promising privacy guarantees without affecting VFL model accuracy. Although this approach is compatible with VT-GAN, its high communication cost makes it less desirable compared to the privacy guarantees already provided by the VT-GAN architecture.

5.3 GANs for Tabular Data

GANs are initially known for its success in image synthesis. However, with its ample application scenarios in areas such as medicine [9] and finance [3], research on GAN for tabular data synthesis also gains attention. Previous research on GANs for tabular data synthesis includes Table-GAN [42], which enhances column dependencies in synthetic data through the use of an auxiliary classification model in conjunction with discriminator training, and CT-GAN [51] and CTAB-GAN [55], which improve data synthesis through preprocessing steps for categorical, continuous, or mixed data types and the use of a conditional vector to reduce mode collapse on minority categories. CTAB-GAN+ [56] and IT-GAN [30] also generate tabular data while protecting the privacy of the original data through the use of differential privacy or by controlling the negative log-density of real records during GAN training. While there have been recent works exploring the use of variational autoencoders (VAE)[51], diffusion models[29], and large language models (LLMs) [4] to synthesize tabular data, GANs remain the most widely used and efficient method in this area. This is what motivates us to incorporate the GAN structure into VFL. Fed-TGAN [54] is the first framework to incorporate a SOTA tabular GAN into a horizontal federated learning system through the use of privacy-preserving feature encoding and table-similarity aware aggregation weights. To the best

of our knowledge, VT-GAN is the first framework to adapt a SOTA conditional tabular GAN for vertical federated learning.

6 CONCLUSION

In this paper, we propose a framework VT-GAN which trains tabular data synthesizer via vertical federated learning. VT-GAN designs a privacy-preserving architecture which allows to train state-ofthe-art tabular GAN with distributed clients where each of them contains unique features. VT-GAN also proposes a training mechanism called training-with-shuffling in order to adopt the conditional vector into tabular GAN training. Results show that VT-GAN can generate synthetic data that capture the column dependencies from different clients, the synthetic data quality is comparable to the one generated by the centralized tabular GAN, as low as to 2.7% difference on machine learning utility. VT-GAN can maintain stable on synthetic data column distribution even under extreme imbalanced data distribution across clients and different number of clients. Differential Privacy (DP) is evaluated on VT-GAN to safeguard against Membership Inference Attacks. The results indicate that DP can effectively protect VT-GAN; however, with a significant cost to the utility of synthetic data. Beyond the presented work, one of the challenges is to investigate measures to counteract collusion between the server and clients. Another interesting area of research is how to defend against data poisoning attacks.

REFERENCES

- Martin Abadi, Andy Chu, Ian Goodfellow, H Brendan McMahan, Ilya Mironov, Kunal Talwar, and Li Zhang. 2016. Deep learning with differential privacy. In Proceedings of the 2016 ACM SIGSAC conference on computer and communications security. 308–318.
- [2] Sercan O Arik and Tomas Pfister. 2019. Tabnet: Attentive interpretable tabular learning. arXiv preprint arXiv:1908.07442 (2019).
- [3] Samuel A. Assefa, Danial Dervovic, Mahmoud Mahfouz, Robert E. Tillman, Prashant Reddy, and Manuela Veloso. 2020. Generating Synthetic Data in Finance: Opportunities, Challenges and Pitfalls. In ICAIF (New York, New York). New York, NY, Article 44, 8 pages. https://doi.org/10.1145/3383455.3422554
- [4] Vadim Borisov, Kathrin Sessler, Tobias Leemann, Martin Pawelczyk, and Gjergji Kasneci. 2023. Language Models are Realistic Tabular Data Generators. In The Eleventh International Conference on Learning Representations. https://openreview. net/forum?id=cEygmQNOeI
- [5] Dingfan Chen, Tribhuvanesh Orekondy, and Mario Fritz. 2020. Gs-wgan: A gradient-sanitized approach for learning differentially private generators. arXiv preprint arXiv:2006.08265 (2020).
- [6] Dingfan Chen, Ning Yu, Yang Zhang, and Mario Fritz. 2020. Gan-leaks: A taxonomy of membership inference attacks against generative models. In Proceedings of the 2020 ACM SIGSAC conference on computer and communications security. 343–362.
- [7] Hao Chen, Kim Laine, and Peter Rindal. 2017. Fast private set intersection from homomorphic encryption. In Proceedings of the 2017 ACM SIGSAC Conference on Computer and Communications Security. 1243–1255.
- [8] Kewei Cheng, Tao Fan, Yilun Jin, Yang Liu, Tianjian Chen, Dimitrios Papadopoulos, and Qiang Yang. 2021. Secureboost: A lossless federated learning framework. IEEE Intelligent Systems 36, 6 (2021), 87–98.
- [9] Edward Choi, Siddharth Biswal, Bradley Malin, Jon Duke, Walter F Stewart, and Jimeng Sun. 2017. Generating multi-label discrete patient records using generative adversarial networks. arXiv preprint arXiv:1703.06490 (2017).
- [10] Changyu Dong, Liqun Chen, and Zikai Wen. 2013. When private set intersection meets big data: an efficient and scalable protocol. In Proceedings of the 2013 ACM SIGSAC conference on Computer & communications security. 789–800.
- [11] Cynthia Dwork, Aaron Roth, et al. 2014. The algorithmic foundations of differential privacy. Foundations and Trends® in Theoretical Computer Science 9, 3–4 (2014), 211–407.
- [12] Wenjing Fang, Derun Zhao, Jin Tan, Chaochao Chen, Chaofan Yu, Li Wang, Lei Wang, Jun Zhou, and Benyu Zhang. 2021. Large-scale secure XGB for vertical federated learning. In Proceedings of the 30th ACM International Conference on Information & Knowledge Management. 443–452.

- [13] Matt Fredrikson, Somesh Jha, and Thomas Ristenpart. 2015. Model inversion attacks that exploit confidence information and basic countermeasures. In Proceedings of the 22nd ACM SIGSAC conference on computer and communications security. 1322–1333.
- [14] Chong Fu, Xuhong Zhang, Shouling Ji, Jinyin Chen, Jingzheng Wu, Shanqing Guo, Jun Zhou, Alex X Liu, and Ting Wang. 2022. Label inference attacks against vertical federated learning. In 31st USENIX Security Symposium (USENIX Security 22), Boston, MA.
- [15] Fangcheng Fu, Xupeng Miao, Jiawei Jiang, Huanran Xue, and Bin Cui. 2022. Towards communication-efficient vertical federated learning training via cacheenabled local updates. In The 46th International Conference on Very Large Data Bases (VLDB).
- [16] Fangcheng Fu, Yingxia Shao, Lele Yu, Jiawei Jiang, Huanran Xue, Yangyu Tao, and Bin Cui. 2021. Vf2boost: Very fast vertical federated gradient boosting for cross-enterprise learning. In Proceedings of the 2021 International Conference on Management of Data. 563–576.
- [17] Fangcheng Fu, Huanran Xue, Yong Cheng, Yangyu Tao, and Bin Cui. 2022. Blindfl: Vertical federated machine learning without peeking into your data. In Proceedings of the 2022 International Conference on Management of Data. 1316–1330.
- [18] Jonas Geiping, Hartmut Bauermeister, Hannah Dröge, and Michael Moeller. 2020. Inverting gradients-how easy is it to break privacy in federated learning? Advances in Neural Information Processing Systems 33 (2020), 16937–16947.
- [19] Robin C Geyer, Tassilo Klein, and Moin Nabi. 2017. Differentially private federated learning: A client level perspective. arXiv preprint arXiv:1712.07557 (2017).
- [20] Ian J. Goodfellow, Jean Pouget-Abadie, Mehdi Mirza, Bing Xu, David Warde-Farley, Sherjil Ozair, Aaron Courville, and Yoshua Bengio. 2014. Generative Adversarial Nets. In Proceedings of the 27th NIPS Volume 2 (Montreal, Canada). Cambridge, MA, USA, 2672–2680.
- [21] Ishaan Gulrajani, Faruk Ahmed, Martin Arjovsky, Vincent Dumoulin, and Aaron Courville. 2017. Improved Training of Wasserstein GANs. In the 31st NIPS (Long Beach, California, USA). 5769–5779.
- [22] Kaiming He, Xiangyu Zhang, Shaoqing Ren, and Jian Sun. 2016. Deep residual learning for image recognition. In Proceedings of the IEEE conference on computer vision and pattern recognition. 770–778.
- [23] Qijian He, Wei Yang, Bingren Chen, Yangyang Geng, and Liusheng Huang. 2020. Transnet: Training privacy-preserving neural network over transformed layer. Proceedings of the VLDB Endowment 13, 12 (2020), 1849–1862.
- [24] Benjamin Hilprecht, Martin Härterich, and Daniel Bernau. 2019. Monte Carlo and Reconstruction Membership Inference Attacks against Generative Models. Proceedings of Privacy Enhancing Technologies 2019, 4 (2019), 232–249.
- [25] Justin Hsu, Marco Gaboardi, Andreas Haeberlen, Sanjeev Khanna, Arjun Narayan, Benjamin C. Pierce, and Aaron Roth. 2014. Differential Privacy: An Economic Method for Choosing Epsilon. In IEEE 27th Computer Security Foundations Symposium, CSF 2014, Vienna, Austria, 19-22 July, 2014. IEEE Computer Society, 398-410. https://doi.org/10.1109/CSF.2014.35
- [26] Aoting Hu, Renjie Xie, Zhigang Lu, Aiqun Hu, and Minhui Xue. 2021. TableGAN-MCA: Evaluating Membership Collisions of GAN-Synthesized Tabular Data Releasing. In Proceedings of the 2021 ACM SIGSAC Conference on Computer and Communications Security. 2096–2112.
- [27] Yaochen Hu, Di Niu, Jianming Yang, and Shengping Zhou. 2019. FDML: A collaborative machine learning framework for distributed features. In Proceedings of the 25th ACM SIGKDD International Conference on Knowledge Discovery & Data Mining. 2232–2240.
- [28] Xiao Jin, Pin-Yu Chen, Chia-Yi Hsu, Chia-Mu Yu, and Tianyi Chen. 2021. CAFE: Catastrophic data leakage in vertical federated learning. Advances in Neural Information Processing Systems 34 (2021), 994–1006.
- [29] Akim Kotelnikov, Dmitry Baranchuk, Ivan Rubachev, and Artem Babenko. 2022. TabDDPM: Modelling Tabular Data with Diffusion Models. arXiv preprint arXiv:2209.15421 (2022).
- [30] Jaehoon Lee, Jihyeon Hyeong, Jinsung Jeon, Noseong Park, and Jihoon Cho. 2021. Invertible Tabular GANs: Killing Two Birds with One Stone for Tabular Data Synthesis. NeurIPS 34 (2021), 4263–4273.
- [31] Oscar Li, Jiankai Sun, Xin Yang, Weihao Gao, Hongyi Zhang, Junyuan Xie, Virginia Smith, and Chong Wang. 2022. Label leakage and protection in two-party split learning. In Proceedings of the 10th International Conference on Learning Representations (ICLR).
- [32] Xiaochen Li, Yuke Hu, Weiran Liu, Hanwen Feng, Li Peng, Yuan Hong, Kui Ren, and Zhan Qin. 2022. OpBoost: A Vertical Federated Tree Boosting Framework Based on Order-Preserving Desensitization. Proc. VLDB Endow. 16, 2 (nov 2022), 202–215. https://doi.org/10.14778/3565816.3565823
- [33] Zitao Li, Bolin Ding, Ce Zhang, Ninghui Li, and Jingren Zhou. 2021. Federated matrix factorization with privacy guarantee. Proceedings of the VLDB Endowment 15, 4 (2021), 900–913.
- [34] Yang Liu, Yingting Liu, Zhijie Liu, Yuxuan Liang, Chuishi Meng, Junbo Zhang, and Yu Zheng. 2020. Federated forest. IEEE Transactions on Big Data (2020).
- [35] Scott M Lundberg and Su-In Lee. 2017. A unified approach to interpreting model predictions. Advances in neural information processing systems 30 (2017).

- [36] Xinjian Luo, Yuncheng Wu, Xiaokui Xiao, and Beng Chin Ooi. 2021. Feature inference attack on model predictions in vertical federated learning. In 2021 IEEE 37th International Conference on Data Engineering (ICDE). IEEE, 181–192.
- [37] Brendan McMahan, Eider Moore, Daniel Ramage, Seth Hampson, and Blaise Aguera y Arcas. 2017. Communication-efficient learning of deep networks from decentralized data. In Artificial intelligence and statistics. PMLR, 1273-1282.
- [38] H Brendan McMahan, Daniel Ramage, Kunal Talwar, and Li Zhang. 2017. Learning differentially private recurrent language models. arXiv preprint arXiv:1710.06963 (2017)
- [39] Payman Mohassel and Peter Rindal. 2018. ABY3: A mixed protocol framework for machine learning. In Proceedings of the 2018 ACM SIGSAC conference on computer and communications security. 35–52.
- [40] Alejandro Mottini, Alix Lheritier, and Rodrigo Acuna-Agost. 2018. Airline passenger name record generation using generative adversarial networks. arXiv preprint arXiv:1807.06657 (2018).
- [41] Mohammad Naseri, Jamie Hayes, and Emiliano De Cristofaro. 2020. Local and central differential privacy for robustness and privacy in federated learning. arXiv preprint arXiv:2009.03561 (2020).
- [42] Noseong Park, Mahmoud Mohammadi, Kshitij Gorde, Sushil Jajodia, Hongkyu Park, and Youngmin Kim. 2018. Data Synthesis Based on Generative Adversarial Networks. Proc. VLDB Endow. 11, 10 (2018), 1071–1083.
- [43] Pengyu Qiu, Xuhong Zhang, Shouling Ji, Tianyu Du, Yuwen Pu, Jun Zhou, and Ting Wang. 2022. Your labels are selling you out: Relation leaks in vertical federated learning. IEEE Transactions on Dependable and Secure Computing (2022).
- [44] Daniele Romanini, Adam James Hall, Pavlos Papadopoulos, Tom Titcombe, Abbas Ismail, Tudor Cebere, Robert Sandmann, Robin Roehm, and Michael A Hoeh. 2021. Pyvertical: A vertical federated learning framework for multi-headed splitnn. arXiv preprint arXiv:2104.00489 (2021).
- [45] Ziteng Sun, Peter Kairouz, Ananda Theertha Suresh, and H Brendan McMahan. 2019. Can you really backdoor federated learning? arXiv preprint arXiv:1911.07963 (2019).

- [46] Amirsina Torfi, Edward A Fox, and Chandan K Reddy. 2020. Differentially Private Synthetic Medical Data Generation using Convolutional GANs. arXiv preprint arXiv:2012.11774 (2020).
- [47] Praneeth Vepakomma, Otkrist Gupta, Abhimanyu Dubey, and Ramesh Raskar. 2019. Reducing leakage in distributed deep learning for sensitive health data. ICLR AI for social good workshop (2019).
- [48] Kang Wei, Jun Li, Chuan Ma, Ming Ding, Sha Wei, Fan Wu, Guihai Chen, and Thilina Ranbaduge. 2022. Vertical federated learning: Challenges, methodologies and experiments. arXiv preprint arXiv:2202.04309 (2022).
- [49] Yuncheng Wu, Shaofeng Cai, Xiaokui Xiao, Gang Chen, and Beng Chin Ooi. 2020. Privacy preserving vertical federated learning for tree-based models. In The 46th International Conference on Very Large Data Bases (VLDB). 2090–2103.
- [50] Liyang Xie, Kaixiang Lin, Shu Wang, Fei Wang, and Jiayu Zhou. 2018. Differentially private generative adversarial network. arXiv preprint arXiv:1802.06739 (2018).
- [51] Lei Xu, Maria Skoularidou, Alfredo Cuesta-Infante, and Kalyan Veeramachaneni. 2019. Modeling Tabular data using Conditional GAN. In NeurIPS.
- [52] Qiang Yang, Yang Liu, Tianjian Chen, and Yongxin Tong. 2019. Federated machine learning: Concept and applications. ACM Transactions on Intelligent Systems and Technology (TIST) 10, 2 (2019), 1–19.
- [53] JianFei Zhang and YuChen Jiang. 2022. A data augmentation method for vertical federated learning. Wireless Communications and Mobile Computing 2022 (2022), 1–16.
- [54] Zilong Zhao, Robert Birke, Aditya Kunar, and Lydia Y Chen. 2021. Fed-TGAN: Federated learning framework for synthesizing tabular data. arXiv preprint arXiv:2108.07927 (2021).
- [55] Zilong Zhao, Aditya Kunar, Robert Birke, and Lydia Y. Chen. 2021. CTAB-GAN: Effective Table Data Synthesizing. In Proceedings of The 13th Asian Conference on Machine Learning, Vol. 157. 97–112. https://proceedings.mlr.press/v157/zhao21a. html
- [56] Zilong Zhao, Aditya Kunar, Robert Birke, and Lydia Y Chen. 2022. CTAB-GAN+: Enhancing Tabular Data Synthesis. arXiv preprint arXiv:2204.00401 (2022).
- [57] Ligeng Zhu, Zhijian Liu, and Song Han. 2019. Deep leakage from gradients. Advances in neural information processing systems 32 (2019).